Vibration in a self-oscillating vocal fold model with left-right asymmetry in body-layer stiffness

Zhaoyan Zhang and zyzhang@ucla.eduAL

Citation: The Journal of the Acoustical Society of America **128**, EL279 (2010); doi: 10.1121/1.3492798
View online: http://dx.doi.org/10.1121/1.3492798
View Table of Contents: http://asa.scitation.org/toc/jas/128/5
Published by the Acoustical Society of America

Vibration in a self-oscillating vocal fold model with left-right asymmetry in body-layer stiffness

Zhaoyan Zhang
UCLA School of Medicine, 31-24 Rehabilitation Center, 1000 Veteran Avenue, Los Angeles, California 90095-1794
zyzhang@ucla.edu

Abstract: This study compares the phonatory behavior of an asymmetric vocal fold model to that of each individual vocal fold model in a hemi-configuration. Although phonation frequencies of the two folds in hemi-configurations had a ratio close to 1:3, a subharmonic synchronization between the two folds was not observed in the asymmetric model. Instead, the vibratory behavior was dominated by the dynamics of one fold only, and the other fold was enslaved to vibrate at the same frequency. Increasing subglottal pressure induced a shift in relative dominance between the two folds, leading to abrupt changes in both vibratory pattern and frequency.

PACS numbers: 43.70.Gr, 43.70.Bk [AL]
Date Received: July 8, 2010 **Date Accepted:** August 27, 2010

1. Introduction

In human phonation, the stiffness or tension of the vocal fold structure is controlled through the activation of laryngeal muscles. When such control of stiffness is lost or weakened in pathological conditions such as unilateral paralysis or paresis, left-right asymmetry in vocal fold stiffness often occurs and leads to alterations and difficulties in voice production. An improved understanding of how such left-right asymmetry in vocal fold stiffness affects vocal fold vibration (e.g., the relative vibration amplitude or phase difference between the two folds) would allow surgeons to better diagnose and treat vocal fold paralysis and paresis.

The influence of left-right stiffness imbalance on vibratory patterns of the vocal folds has been the focus of many previous studies. Using an asymmetric two-mass model, Ishizaka, Isshiki, and colleagues (Ishizaka and Isshiki, 1976; Isshiki *et al.*, 1977) showed that, for large glottal openings, both 1:1 entrainment (normal phonation) and higher-order entrainment such as 1:2 or 2:2 entrainments (subharmonics) between the left and right folds can occur for certain conditions of the subglottal pressure and vocal fold parameters. Steinecke and Herzel (1995) further pointed out that the origin of different instabilities or vibratory regimes (e.g., subharmonics, biphonation, and chaotic vibrations) can be traced back to the desynchronization of two oscillators, the left and right folds. Such desynchronization occurred for sufficiently large subglottal pressures and large asymmetry in eigenfrequencies between the two folds.

In this study, such synchronization or interaction of two vocal fold models with different body-layer stiffness was investigated by comparing vibratory behavior of an asymmetric model to that of each individual component fold in a hemi-configuration.

For this purpose, physical models with well-controlled geometry and directly measurable material properties were used. Compared to computational models, physical models allow a better representation of phonatory physics. With high repeatability, physical models also make it possible to perform repeatable and systematic parametric studies, thus providing valuable insights into the phonatory process. In this study, two physical models of the vocal fold with different body-cover stiffness ratios were used: one with a body-cover stiffness ratio of one, and the other with an extremely large body-cover stiffness ratio. The focus was to understand how dynamical differences in these two models affect the phonatory and vibratory behavior of the asymmetric vocal fold model formed by these two physical models with different body-layer stiffnesses.

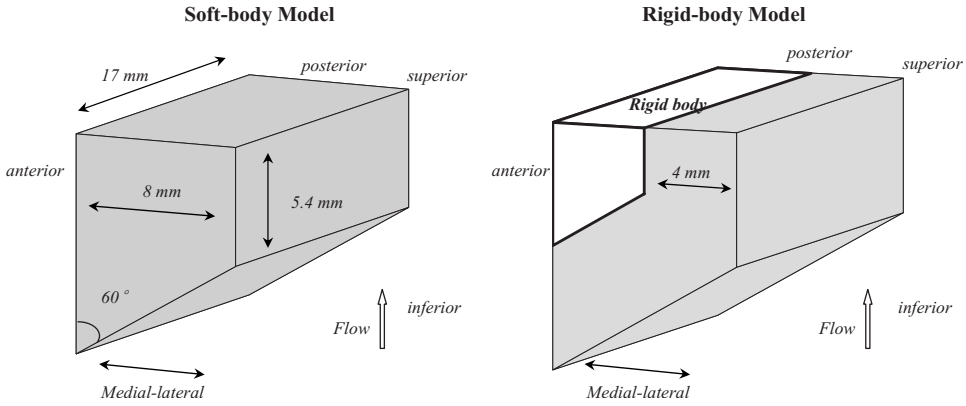

Fig. 1. Sketches of the soft-body model (left) and the rigid-body model (right) used in this study.

2. Experimental procedure

The experimental setup was similar to that used in previous studies (Zhang *et al.*, 2006, 2009). More details of the setup can be found in these previous studies. The setup consisted of an expansion chamber (with a rectangular cross-section of the dimension 23.5 × 25.4 and 50.8-cm long) simulating the lungs, a 13-cm straight circular PVC tube (inner diameter of 2.54 cm) simulating the tracheal tube, and a rubber model of the vocal folds. No vocal tract was used in this study. The vocal fold models were made by mixing a two-component liquid polymer solution (Evergreen 10, Smooth On, Inc.) with a liquid flexibilizer solution (Everflex). Two models were used in this study, as shown in Fig. 1. The first model was essentially a single-layer isotropic model, and had the same geometry as the ones used in previous studies (Zhang *et al.*, 2006). The Young's modulus was about 6.5 kPa as measured using the indentation method with an indenter diameter of 1 mm and an indentation depth of 1 mm. Within the body-cover framework of the vocal fold structure (Hirano, 1974), this model corresponds to a two-layer vocal fold model with a body-cover stiffness ratio of one. In this study, this model is denoted as the soft-body model. The second model consisted of a thin cover-layer of 4-mm thickness mounted on a rigid acrylic sublayer, with an overall geometry the same as the soft-body model. Conceptually, this model corresponds to a two-layer model with an extremely large body-cover stiffness ratio (about 10 000). In this study, this model is denoted as the rigid-body model. The cover layer of the rigid-body model had identical material properties as the soft-body model.

Clinically, the rigid-body model resembles the normal vocal condition with strong activation of the thyroarytenoid muscle (Hirano, 1974), which leads to a body layer much stiffer than the cover layer. In contrast, the soft-body model resembles a condition when the body layer is as soft as the cover layer, due to either inactivation of the thyroarytenoid muscle or as in a paralyzed vocal fold (Hirano, 1974). Note that the resting glottal opening was almost zero for all conditions examined in this study, which is in contrast to large glottal opening as often observed in vocal fold paralysis.

Two sets of experiments were conducted in this study. In the first set of experiments, the phonatory characteristics of individual models were studied in a hemi-model configuration, i.e., pairing each model with a rigid plate (e.g., Zhang *et al.*, 2006). In the second set of experiments, an asymmetric vocal fold model was created by combining the two models to form a glottis. The phonatory behavior of the asymmetric model was then studied and compared to those in hemi-model conditions.

For each set of experiments, the flow rate was increased in discrete increments from zero to a value above onset, and then decreased back to zero in discrete decrements. At each step, after a delay of about 2–3 s after the flow rate change, the mean subglottal pressure, mean flow rate, and acoustic pressure inside the tracheal tube and downstream the glottis were measured for a 1-s period. This procedure allows identification of phonation onset and regimes of

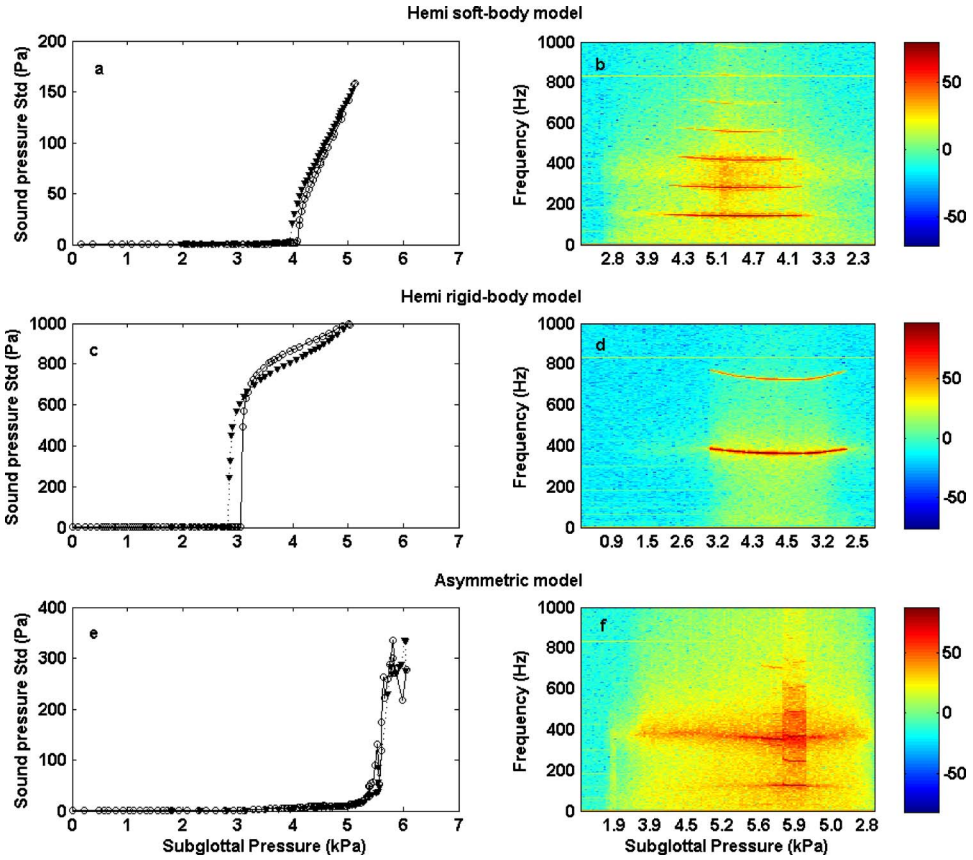

Fig. 2. (Color online) The amplitude (left column) and power spectra (right column) of the subglottal acoustic pressure as a function of increasing and decreasing subglottal pressure for the soft-body model in a hemi-model configuration (first row), the rigid-body model in a hemi-model configuration (second row), and the asymmetric vocal fold model (last row). In the sound pressure amplitude plots on the left column, ○ denotes data obtained for increasing subglottal pressure; ▼ denotes data obtained for decreasing subglottal pressure.

distinct vibratory behavior. For hemi-configuration experiments, the medial surface vibration of the vocal fold was recorded using a high-speed digital camera (Fastcam-Ultima APX) at 2000 frames per second and an image resolution of 1024×1024 pixels (Zhang *et al.*, 2006).

3. Results in hemi-model experiments

Figure 2 (first two rows) shows the amplitudes and spectra of the subglottal acoustic pressure as a function of the mean subglottal pressure for the two vocal fold models in a hemi-model configuration. For the soft-body model [Figs. 2(a) and 2(b)], phonation onset occurred at a subglottal pressure of approximately 4.12 kPa and at a frequency of 145 Hz. Beyond onset the phonation frequency changed only slightly with the subglottal pressure. For the rigid-body model [Figs. 2(c) and 2(d)], phonation onset occurred at a subglottal pressure of approximately 3.08 kPa and at a frequency of 384 Hz. The variation of phonation frequency with the subglottal pressure was also small. For both cases, phonation onset was accompanied by a sudden increase in the amplitude of the subglottal acoustic pressure. Note that hysteresis was observed in both models, with phonation onset pressure slightly higher than phonation offset pressure.

Figure 3 compares the medial surface vibration pattern for the two vocal fold models as imaged in the hemi-model configuration at subglottal pressures slightly above onset.

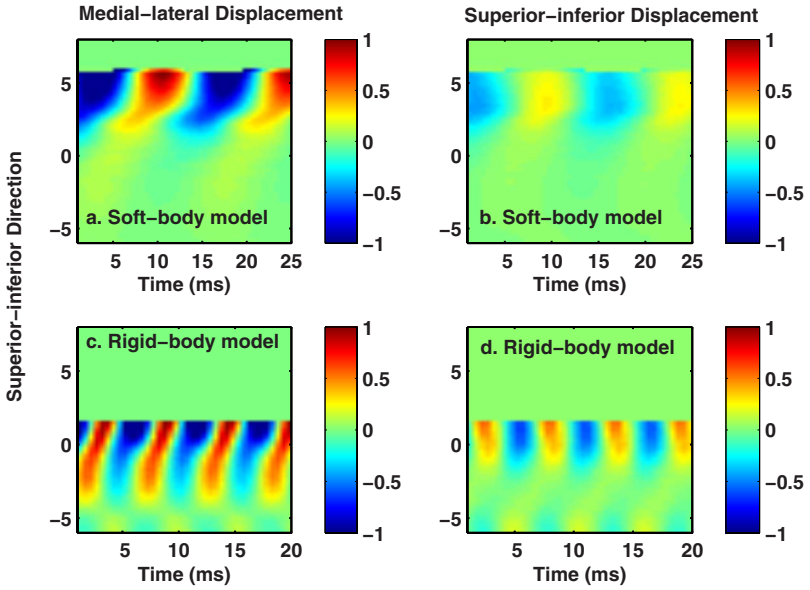

Fig. 3. (Color online) Spatiotemporal plots of the medial-lateral (left column) and superior-inferior (right column) components of the vocal fold surface displacement for a coronal slice of the soft-body model (top row) and rigid-body model (bottom row) in a hemi-model configuration. The abscissa is time, and the ordinate is the spatial location in the superior-inferior direction, with increasing values in the superior direction. The coronal slice was taken at the midpoint between anterior and posterior extremes.

The vibration displacement of a coronal slice of the medial surface was plotted as a function of time (abscissa) and location in the superior-inferior direction along the medial surface (ordinate). The rigid-body model exhibited a more wave-like motion, as demonstrated by the continuous phase change in the medial-lateral motion along the upper portion of the medial surface. In contrast, the soft-body model showed a dominant in-phase medial-lateral motion along the upper portion of the medial surface, as demonstrated by the vertical orientation of iso-amplitude contours. This difference in the medial-lateral displacement field between a rigid-body model and a soft-body model is consistent with the prediction of Zhang (2009) (compare Fig. 2 of this study to Fig. 5 of Zhang, 2009). Similar observation was also reported in the clinic (Fex and Elmqvist, 1973; Hirano, 1974).

Due to a phonation frequency close to the first subglottal resonance (around 375 Hz with a quality factor of about 4.4), the rigid-body model also exhibited a large in-phase inferior-superior motion along the medial surface, in contrast to a much reduced inferior-superior motion in the soft-body model. This difference in the excitation of inferior-superior motion is consistent with previous experimental observations regarding the influence of subglottal acoustics on phonation (Zhang *et al.*, 2009). The strong influence of the subglottal acoustics also led to a low phonation threshold pressure in the hemi rigid-body model.

For the same subglottal pressure, the flow rate was much higher (nearly doubled) in the soft-body model than in the rigid-body model. This indicates a much larger mean glottal opening for the soft-body model than the rigid-body model, which is consistent with the observation in Ruty *et al.* (2006) and Pickup and Thomson (2009).

4. Results in asymmetric-model experiments

Figures 2(e) and 2(f) show the amplitudes and spectra of the subglottal acoustic pressure as a function of the mean subglottal pressure in the asymmetric vocal fold model formed by pairing the soft-body model with the rigid-body model. Two regimes of distinct vibratory patterns can be identified as the subglottal pressure was gradually increased. At low subglottal pressures,

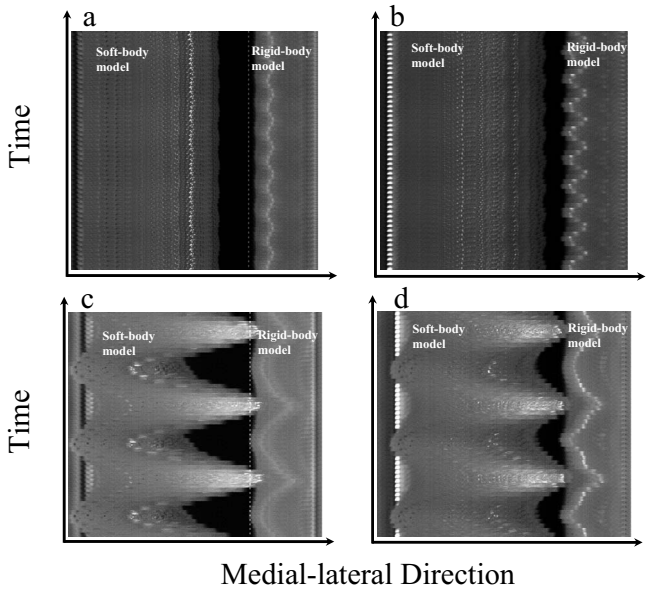

Fig. 4. Time history of a medial-lateral image slice of the asymmetrical vocal folds from a superior view. (a) First vibratory regime, the slice was taken from the middle in the anterior-posterior direction, (b) first vibratory regime, the slice was taken from the anterior quarter in the anterior-posterior direction, (c) second vibratory regime, the slice was taken from the middle in the anterior-posterior direction, and (d) second vibratory regime, the slice was taken from the anterior quarter in the anterior-posterior direction.

phonation started at around 5.37 kPa with a phonation frequency of 360 Hz. Unlike the two hemi-model cases, no sudden increase in sound pressure amplitude was observed at phonation onset. The second vibratory regime started around 5.98 kPa, with a phonation frequency of about 125 Hz. The transition between the two regimes was accompanied by a sudden increase in sound pressure amplitude. After the transition, the sound pressure amplitude was much larger than that in the hemi soft-body model but still smaller than the amplitude above onset in the hemi rigid-body model.

The phonation frequency in the first regime (360 Hz) was close to the phonation frequency observed in the hemi rigid-body model (384 Hz). This suggests that vibration in the first regime was dominated by the dynamics of the rigid-body model. Indeed, this was confirmed by the observed vibration pattern as shown in Figs. 4(a) and 4(b). Figures 4(a) and 4(b) show the image of two medial-lateral slices of the superior surface of the asymmetric vocal fold model as a function of time (ordinate). The two slices were located at the middle [Fig. 4(a)] and the anterior quarter [Fig. 4(b)] in the anterior-posterior direction, respectively. Although neither model was strongly excited, the rigid-body model clearly vibrated at a much larger amplitude than the soft-body model. The two models seemed to vibrate in phase with each other, with only a slight phase difference.

On the other hand, vibration in the second regime was dominated by the dynamics of the soft-body model, as shown in Figs. 4(c) and 4(d), with a phonation frequency (about 125 Hz) close to that observed in the hemi soft-body model (145 Hz). The soft-body model was strongly excited and had a maximum vibration amplitude (about 6 mm) comparable to its depth in the medial-lateral direction. The rigid-body model exhibited only small-amplitude vibration and seemed to be driven by the soft-body model. The natural modes of rigid-body model (with a frequency about three times that of the phonation frequency) were only excited immediately following the impact, which led to the high-frequency fluctuation in the otherwise sinusoidal waveform in Fig. 4(d). But this excitation was weak and quickly damped out before the next impact came in. Such large contrast in amplitude between the two folds also rules out the pos-

sibility of a 1:3 synchronization between the two folds. As the rigid-body model was largely driven by the motion of the soft-body model, the two models vibrated nearly 180° out of phase with each other. Note that the vibratory pattern in this regime is similar to observations in canine larynxes with recurrent laryngeal nerve paralysis (Moore *et al.*, 1987).

5. Discussions

Considering that the phonation frequencies of the two folds in hemi-configurations had a ratio close to 1:3, a subharmonic synchronization between the two folds with a frequency ratio of 1:3 seemed likely but was not observed in the experiment. Instead, the two folds were synchronized to vibrate at the same frequency in both regimes. It appears that the two folds, or the two fluid-structure interactions between airflow and each of the two folds, were competing for dominance in the asymmetric model. At low subglottal pressure, the relative strength between these two fluid-structure interactions can be reasonably quantified by comparing the phonation threshold pressures of the two models as measured in the hemi-configuration. Thus the rigid-body model, with a lower phonation threshold pressure due to its coupling to the subglottal acoustics, was able to dominate and induce phonation onset at low subglottal pressures. The soft-body model contributed only by inducing a large overall glottal opening in the asymmetric model and thus weakening coupling strength between airflow and the rigid-body model.

However, increasing subglottal pressure was able to change the relative dominance between the two folds. And the soft-body model, despite a high phonation threshold pressure in the hemi-configuration, was able to overcome the rigid-body model and dominate in the second regime. The exact mechanism underlying this transition is not clear. It could be that the coupling of the rigid-body model to subglottal acoustics was weakened at high subglottal pressures. Or changes in certain dynamical variables such as the glottal opening may have changed the relative strength between the two fluid-structure interactions. Note that similar shift in vocal fold vibration pattern from one type to another, or register change, due to slight changes in parameters of the vocal system was also reported in previous studies (Ishizaka and Isshiki, 1976; Tokuda *et al.*, 2007).

Although considerable work has been done toward understanding the interaction between the two folds in various conditions of stiffness imbalance (Ishizaka and Isshiki, 1976; Smith *et al.*, 1992; Steinecke and Herzel, 1995), the results of this study show that further studies are needed to understand the general principles underlying the synchronization (both 1:1 and subharmonic synchronization) of the two folds in an asymmetric vocal fold model with more realistic geometrical and biomechanical properties. In vocal fold paralysis, stiffness asymmetry is often accompanied by large resting glottal opening, which may affect the relative strength between different eigenmode synchronizations (both same-fold and cross-fold synchronization) and lead to completely different vibratory behavior (Ishizaka and Isshiki, 1976). Experiments are currently under way with well-controlled and systematic variations in vocal fold geometry, stiffness, and glottal opening, in order to map out regions of distinct vibratory patterns in the parameter space, and identify factors that determine amplitude and phase difference, and frequency of the resulting vocal fold vibration.

Acknowledgments

The author thanks Dr. J Neubauer for his assistance in imaging medial surface vibration. This study was supported by Research Grant Nos. R01 DC009229 and R01 DC003072 from NIDCD, NIH.

References and links

Fex, S., and Elmqvist, D. (**1973**). "Endemic recurrent laryngeal nerve paresis," Acta Oto-Laryngol. **75**, 368–369.
Hirano, M. (**1974**). "Morphological structure of the vocal cord as a vibrator and its variations," Folia Phoniatr (Basel) **26**, 89–94.
Ishizaka, K., and Isshiki, N. (**1976**). "Computer simulation of pathological vocal-cord vibration," J. Acoust. Soc. Am. **60**, 1193–1198.
Isshiki, N., Tanabe, M., Ishizaka, K., and Broad, D. (**1977**). "Clinical significance of asymmetrical vocal cord tension," Ann. Otol. Rhinol. Laryngol. **86**, 58–66.
Moore, D. M., Berke, G. S., Hanson, D. G., and Ward, P. H. (**1987**). "Videostroboscopy of the canine larynx: The

effects of asymmetric laryngeal tension," Laryngoscope **97**, 543–553.
Pickup, B. A., and Thomson, S. L. (**2009**). "Influence of asymmetric stiffness on the structural and aerodynamic response of synthetic vocal fold models," J. Biomech. **42**, 2219–2225.
Ruty, N., Van Hirtum, A., Pelorson, X., Hirschberg, A., and Lopez, I. (**2006**). "A preliminary study of asymmetric vocal folds vibrations: Modeling and in-vitro validation," in 7th International Seminar on Speech Production (ISSP7), Ubatuba, Brazil, pp. 61–68, http://www.cefala.org/issp2006/cdrom/main_index.html (Last viewed 09/16/2010).
Smith, M. E., Berke, G. S., Gerratt, B. R., and Kreiman, J. (**1992**). "Laryngeal paralyses: Theoretical considerations and effects on laryngeal vibration," J. Speech Hear. Res. **35**, 545–554.
Steinecke, I., and Herzel, H. (**1995**). "Bifurcations in an asymmetric vocal fold model," J. Acoust. Soc. Am. **97**, 1874–1884.
Tokuda, I. T., Horacek, J., Svec, J. G., and Herzel, H. (**2007**). "Comparison of biomechanical modeling of register transitions and voice instabilities with excised larynx experiments," J. Acoust. Soc. Am. **122**, 519–531.
Zhang, Z. (**2009**). "Characteristics of phonation onset in a two-layer vocal fold model," J. Acoust. Soc. Am. **125**, 1091–1102.
Zhang, Z., Neubauer, J., and Berry, D. A. (**2006**). "Aerodynamically and acoustically-driven modes of vibration in a physical model of the vocal folds," J. Acoust. Soc. Am. **120**, 2841–2849.
Zhang, Z., Neubauer, J., and Berry, D. A. (**2009**). "Influence of vocal fold stiffness and acoustic loading on flow-induced vibration of a single-layer vocal fold model," J. Sound Vib. **322**, 299–313.